Journal of Power Sources 196 (2011) 8073–8084

Contents lists available at ScienceDirect

Journal of Power Sources

journal homepage: www.elsevier.com/locate/jpowsour

Effects of different electrode materials on the performance of lithium tetrafluorooxalatophosphate (LiFOP) electrolyte

Liu Zhou, Swapnil Dalavi, Mengqing Xu, Brett L. Lucht*

Department of Chemistry, University of Rhode Island, 51 Lower College Rd., Kingston, RI 02881, USA

ARTICLE INFO

Article history:
Received 25 March 2011
Received in revised form 27 April 2011
Accepted 28 April 2011
Available online 13 May 2011

Keywords:
Lithium ion battery
Electrolyte
Surface analysis

ABSTRACT

The cycling performance of $LiPF_4(C_2O_4)$ electrolyte is compared with $LiPF_6$ electrolyte in the presence of several different electrode materials. The cycling of MCMB/$LiNi_{1/3}Co_{1/3}Mn_{1/3}O_2$ and natural graphite/$LiFePO_4$ cells provides very similar performance for both electrolytes. However, MCMB/$LiMn_2O_4$ cells have a lower initial reversible capacity with $LiPF_4(C_2O_4)$ electrolytes. A detailed analysis of the surface films on both the cathode and the anode via X-ray photoelectron spectroscopy (XPS) and scanning electron microscopy (SEM) was conducted. The performance differences are attributed to the anode as opposed to the cathode.

1. Introduction

Lithium-ion batteries are very interesting due to their high energy density. While the incorporation of lithium-ion batteries into portable electronic devices has been occurring for over a decade, incorporation of LIB into electric vehicles is just beginning. Unfortunately, currently available lithium-ion batteries do not satisfy some of the performance goals for electric vehicles due to loss of power and capacity upon storage or prolonged use, especially at moderately elevated temperatures (>55 °C). The electrolytes used in commercial lithium-ion batteries are composed of $LiPF_6$ dissolved in organic carbonates or esters [1]. The performance degradation is linked to the poor thermal stability of $LiPF_6$ and the reactions of the electrolyte with the surface of the electrode materials [2–5]. Many research groups have attempted to develop new electrolyte formulations through the incorporation of electrolyte additives designed to generate a more stable solid electrolyte interphase (SEI) on the anode and improve cell resilience to high temperatures [6]. There have also been investigations on the development of alternative salts for lithium ion battery electrolytes [1]. In particular, lithium bisoxalatoborate (LiBOB) [7,8] has received significant attention. However, none of the reported salts have properties superior to $LiPF_6$.

We have been conducting a detailed analysis of a novel salt, lithium tetrafluorooxalatophosphate [$LiPF_4(C_2O_4)$], which shows many comparable properties with $LiPF_6$, including ionic conductivity, electrochemical stability window, and cycling stability [9–11]. However, $LiPF_4(C_2O_4)$ has much better thermal and hydrolytic stability and performance retention upon accelerated aging. This unique combination of properties makes $LiPF_4(C_2O_4)$ an interesting alternative to $LiPF_6$. In this work, we have expanded our investigation of $LiPF_4(C_2O_4)$ electrolyte, to include multiple types of electrode materials (cathode and anode). The performance in cells cycled at room temperature has been investigated by electrochemical cycling. In order to develop a better understanding of the sources of performance differences between $LiPF_4(C_2O_4)$ and $LiPF_6$, the surfaces of the electrodes have been analyzed after cycling.

2. Experimental

A standard electrolyte composed of 1.2 M of lithium hexafluorophosphate ($LiPF_6$) in 3:7 EC/EMC (vol.) was obtained from Novolyte Corporation and used without further purification ($LiPF_6$ electrolyte). Lithium tetrafluorooxalatophosphate, $LiPF_4(C_2O_4)$, was synthesized as described previously[10]. $LiPF_4(C_2O_4)$ was dissolved in EC/EMC (3:7, vol.) to generate the $LiPF_4(C_2O_4)$ electrolyte (LiFOP electrolyte).

Coin cells were fabricated in a glove box with argon of high purity. The anode of MCMB/$LiNi_{1/3}Co_{1/3}Mn_{1/3}O_2$ cells is made of 88.8% mesocarbon microbeads (MCMB), 8% of poly(vinylidene difloride) (PVDF) binder, and 3.2% of acetylene black. The cathode is composed of 80% $LiNi_{1/3}Co_{1/3}Mn_{1/3}O_2$ active material, 10% PVDF, and 10% conductive material. The anodes of lithium iron phosphate ($LiFePO_4$) cells contain natural graphite (NG) with CMS binder and the cathodes contain lithium iron phosphate powder with PVDF binder and were obtained from MTI. The cathodes of

* Corresponding author. Tel.: +1 401 874 5071; fax: +1 401 874 5072.
E-mail address: blucht@chm.uri.edu (B.L. Lucht).

0378-7753/$ – see front matter © 2011 Elsevier B.V. All rights reserved.
doi:10.1016/j.jpowsour.2011.04.061

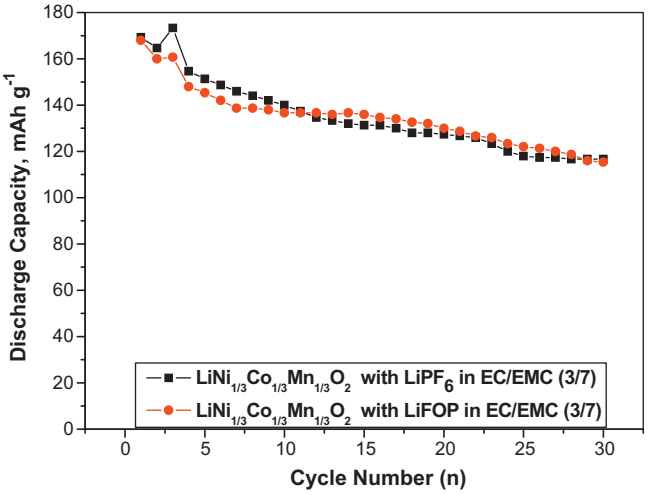

Fig. 1. Cycling performance of $LiPF_6$ and LiFOP electrolytes in MCMB/$LiNi_{1/3}Co_{1/3}Mn_{1/3}O_2$ cells.

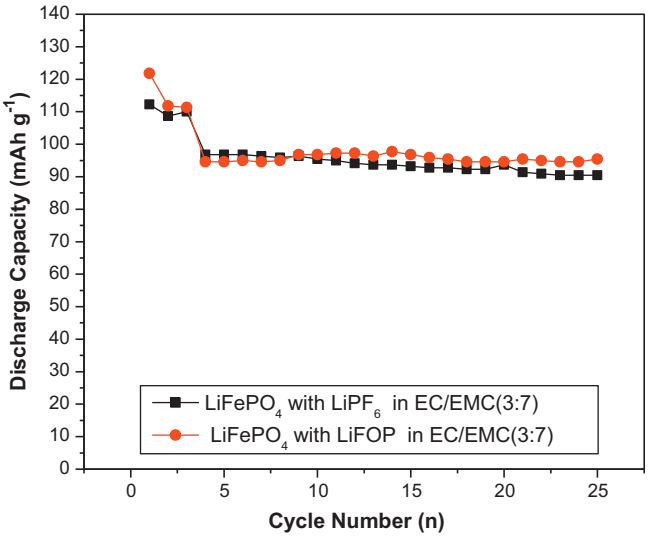

Fig. 2. Cycling performance of $LiPF_6$ and LiFOP electrolytes in natural graphite/$LiFePO_4$ cells.

MCMB/$LiMn_2O_4$ cells contain 81.6% of lithium manganese oxide, 8% of PVDF binder, 6.4% of acetylene black and 4% of graphite. The anode of MCMB/$LiMn_2O_4$ cells is made of 85.6% MCMB, 8% of PVDF binder, and 4% of acetylene black. Between each anode and cathode there is a polypropylene separator which contains 30 μL of electrolyte. The coin cells were cycled with a constant current–constant voltage charge and a constant current discharge between 4.1 V and 3.0 V using an Arbin Instrument battery cycler. The cells were cycled with the following formation procedures: first cycle at *C*/20, second and third cycle at *C*/10 and remaining two cycles at *C*/5. After the initial five formation cycles the cells were cycled at a *C*/5 rate for 20 cycles. Multiple cells of each type were constructed and cycled with good reproducibility.

The cells were opened in an Ar glove box after cycling and the electrodes were extracted for surface analysis. The electrodes were rinsed with DMC three times prior to surface analysis. The XPS spectra were acquired with a PHI 5500 system using Al Kα radiation ($h\nu$ = 1486.6 eV) under ultra high vacuum. Characterization of XPS peaks was made by recording XPS spectra for reference compounds, which would be present on the electrode surfaces: LiF, Li_2CO_3, $Li_xPO_yF_z$ and lithium alkylcarbonate. The graphite peak at 284.3 eV was used as a reference for the final adjustment of the energy scale in the spectra. Lithium was not monitored due to its low inherent sensitivity and small change of binding energy. The spectra obtained were analyzed by Multipak 6.1A software and fitting using XPS peak software (version 4.1). A mixture of Lorentzian and Gaussian functions was used for the least-squares curves fitting procedure. Scanning electron microscopy (SEM) images were taken on a JEOL 5900 scanning electron microscope.

3. Results and discussion

3.1. Cycling performance

3.1.1. Cycling performance of MCMB/$LiNi_{1/3}Co_{1/3}Mn_{1/3}O_2$ cells

Lithium-ion coin cells were constructed containing $LiPF_6$ and LiFOP electrolytes and MCMB/$LiNi_{1/3}Co_{1/3}Mn_{1/3}O_2$ electrodes. Upon initial formation cycles the cells containing LiFOP electrolyte have very similar cycling performance to the cells containing $LiPF_6$ electrolyte (Fig. 1). In addition, the first cycle coulombic efficiency of cells with LiFOP electrolyte is high (73%) and comparable to the cells containing $LiPF_6$ (71%).

3.1.2. Cycling performance of graphite/$LiFePO_4$ cells

Lithium-ion coin cells were constructed containing $LiPF_6$ and LiFOP electrolytes and graphite/$LiFePO_4$ electrodes. Upon initial formation cycles the cells containing LiFOP electrolyte had very similar capacity to the cells containing $LiPF_6$ electrolyte (Fig. 2). The first cycle coulombic efficiency of cells with LiFOP electrolyte is very high (87%) and comparable to the cells containing $LiPF_6$ (82%).

3.1.3. Cycling performance of MCMB/$LiMn_2O_4$ cells

Lithium-ion coin cells were constructed containing $LiPF_6$ and LiFOP electrolytes and MCMB/$LiMn_2O_4$ electrodes. Upon initial formation cycles the cells containing LiFOP electrolyte had significantly less capacity (38 mAh/g) than the cells containing $LiPF_6$ electrolyte (99 mAh/g). The first cycle efficiency for the MCMB/$LiMn_2O_4$ cells with LiFOP electrolyte is only 33% compared to 83% for the cells containing $LiPF_6$ electrolyte. However, after the initial formation cycles the coulombic efficiency of cells with LiFOP electrolyte is high and comparable to the cells containing $LiPF_6$ (Fig. 3).

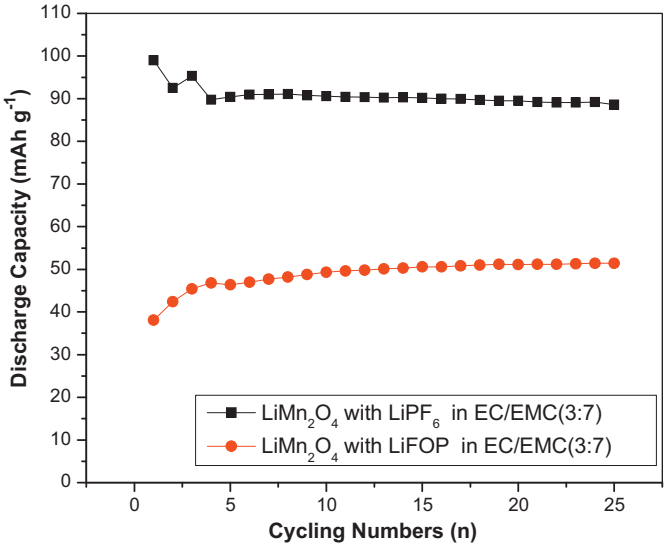

Fig. 3. Cycling performance of $LiPF_6$ and LiFOP electrolytes in MCMB/$LiMn_2O_4$ cells.

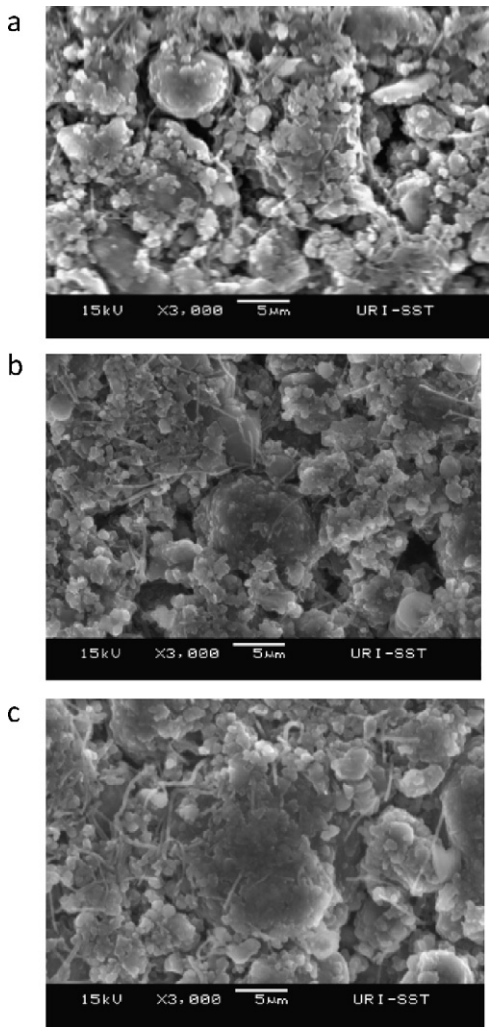

Fig. 4. SEM images of MCMB graphite anode (a) fresh, (b) cycled with $LiPF_6$ electrolyte and (c) cycled with LiFOP electrolyte cycled with a $LiNi_{1/3}Co_{1/3}Mn_{1/3}O_2$ cathode.

3.2. SEM images

The SEM images of a MCMB graphite anode paired with a $LiNi_{1/3}Co_{1/3}Mn_{1/3}O_2$ cathode (a) fresh; (b) cycled with $LiPF_6$ electrolyte; and (c) cycled with LiFOP electrolyte are depicted in Fig. 4. There are only small changes occurring to the surface of these anodes after 20 cycles. The surface of the anode materials after cycling with either electrolyte contains a thin amorphous coating consistent with the formation of an SEI [1,3]. However, the surface coverage is very similar for both electrolytes.

The SEM images of a $LiNi_{1/3}Co_{1/3}Mn_{1/3}O_2$ cathode (a) fresh; (b) cycled with $LiPF_6$ electrolyte; and (c) cycled with LiFOP electrolyte are provided in Fig. 5. There are no detectable changes to the surface of these cathodes after 20 cycles. The lack of observed changes on the surface of the cathode is consistent with thinner surface films as typically observed for lithium ion cells [2].

Table 1
Elemental analysis of MCMB graphite anode used for $LiNi_{1/3}Co_{1/3}Mn_{1/3}O_2$ cathode.

	C 1s (%)	O 1s (%)	F 1s (%)	P 2p (%)
Fresh MCMB	68.6	1.1	30.3	0
$LiPF_6$	39.5	20.6	37.3	2.6
LiFOP	39.2	40.9	13.8	6.1

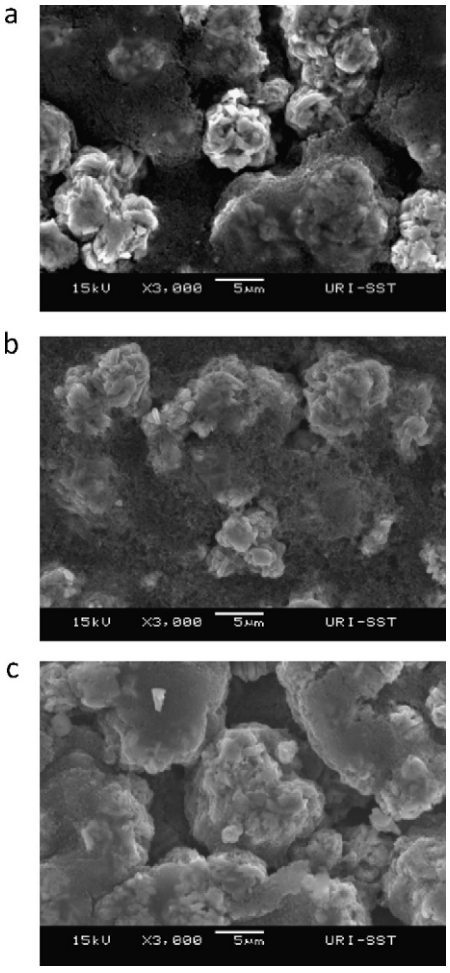

Fig. 5. SEM images of $LiNi_{1/3}Co_{1/3}Mn_{1/3}O_2$ cathode (a) fresh, (b) cycled with $LiPF_6$ electrolyte and (c) cycled with LiFOP electrolyte.

The SEM images of natural graphite (NG) anode with a $LiFePO_4$ cathode (a) fresh; (b) cycled with $LiPF_6$ electrolyte; (c) cycled with LiFOP electrolyte are depicted in Fig. 6. Unlike the spherical MCMB particles the graphite particles in these cells are rod shaped with a smooth surface. After cycling with the baseline electrolyte (1.2 M $LiPF_6$ in 3:7 EC:EMC, vol.), there are significant changes to the surface of the particles. The surface of the anode is much rougher and appears to be covered with thick surface film. This film suggests the presence of an anode SEI. The surface of the anode cycled with the LiFOP electrolyte (1.2 M LiFOP in 3:7 EC:EMC, vol.) has similar changes. The smooth surface is covered with a thick amorphous layer consistent with the generation of an anode SEI.

Fig. 7 contains the SEM images of a $LiFePO_4$ cathode (a) fresh; (b) cycled with $LiPF_6$ electrolyte; and (c) cycled with LiFOP electrolyte. There are no apparent changes to the surface of these cathodes after 20 cycles. The surface morphology is retained.

The SEM images of a MCMB anode with a $LiMn_2O_4$ cathode (a) fresh; (b) cycled with $LiPF_6$ electrolyte; and (c) cycled with LiFOP electrolyte are provided in Fig. 8. The MCMB particles of this anode material are larger and more uniform than the MCMB anodes used for the NCM cells. The changes to the anode surface are smaller than observed for the previous anode materials upon cycling with either electrolyte. While the surface roughness of the smaller graphite particles appears to have been lessened due to the formation of surface films, the larger particles appear largely unchanged. However, the surface films generated in both the $LiPF_6$ electrolyte and the LiFOP electrolyte appear very similar.

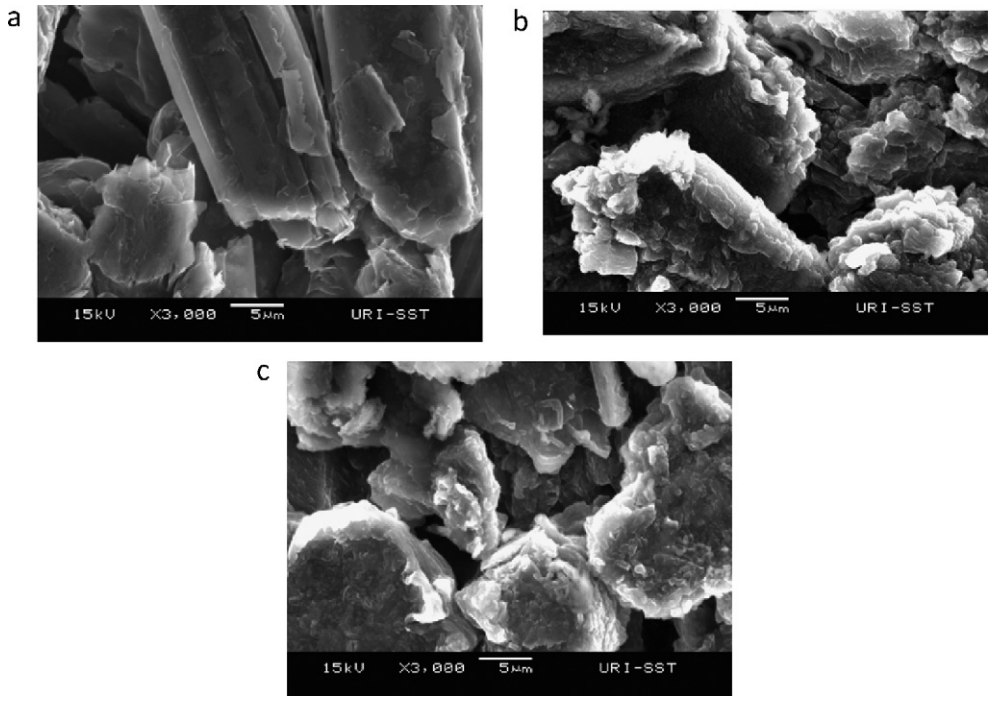

Fig. 6. SEM images of natural graphite anode (a) fresh, (b) cycled with $LiPF_6$ electrolyte and (c) cycled with LiFOP electrolyte with a $LiPePO_4$ cathode.

The SEM images of a $LiMn_2O_4$ cathode (a) fresh; (b) cycled with $LiPF_6$ electrolyte; and (c) cycled with LiFOP electrolyte are depicted in Fig. 9. The surfaces of the $LiMn_2O_4$ cathodes are very similar before and after cycling with either electrolyte.

3.3. XPS analysis

The XPS spectra of MCMB graphite anode paired with a $LiNi_{1/3}Co_{1/3}Mn_{1/3}O_2$ cathode (a) fresh; (b) cycled with $LiPF_6$ electrolyte; and (c) cycled with LiFOP electrolyte are shown in Fig. 10. There are three peaks in C 1s spectrum of the fresh MCMB anode, graphite peak at 284.3 eV, peaks of PVdF at 285.7 eV and 290.4 eV, respectively. The peak at 532.5 eV in O 1s spectrum is characteristic of surface oxidation (CO_2^-) of the electrode. The F 1s spectrum contains a peak characteristic of PVdF at 687.6 eV.

Surface analysis of the anode after cycling with $LiPF_6$ electrolyte (1.2 M $LiPF_6$ in EC/EMC, 3:7, vol.) indicates that the concentration of carbon is decreased, while the concentrations of oxygen, fluorine

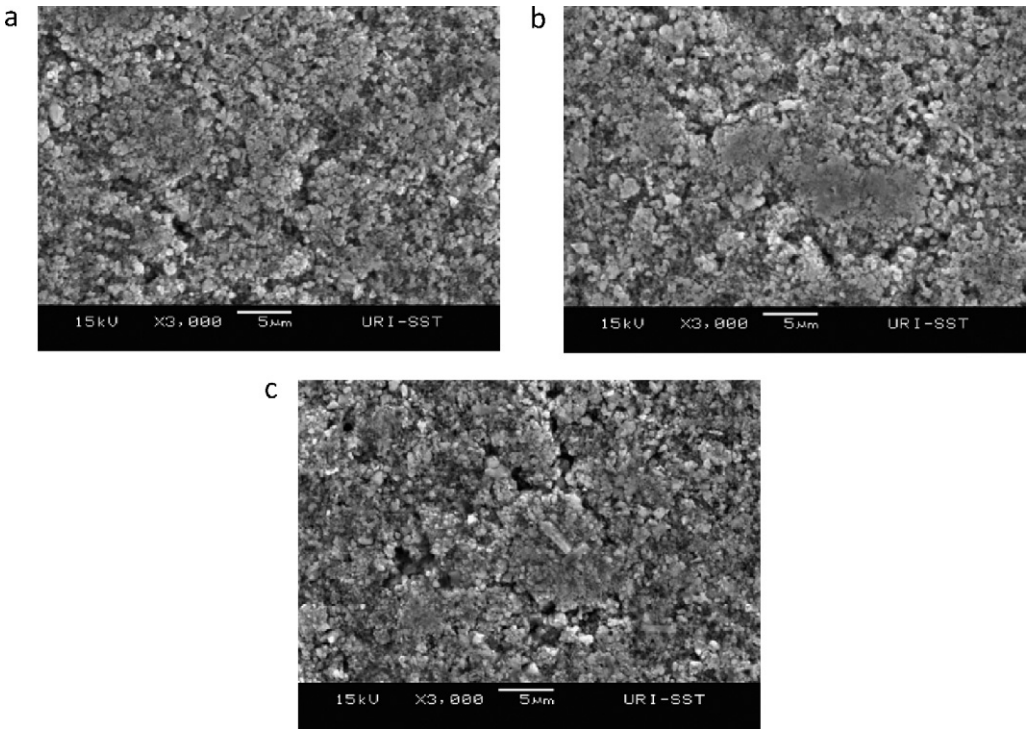

Fig. 7. SEM images of $LiFePO_4$ cathode (a) fresh, (b) cycled with $LiPF_6$ electrolyte and (c) cycled with LiFOP electrolyte.

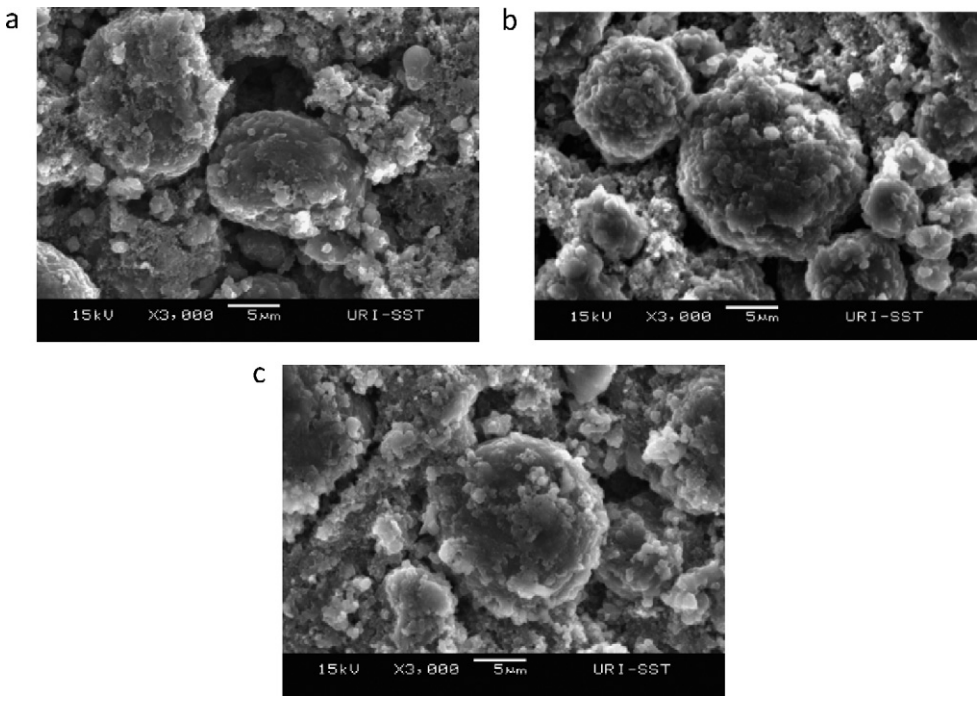

Fig. 8. SEM images of a MCMB anodes (a) fresh, (b) cycled with $LiPF_6$ electrolyte and (c) cycled with LiFOP electrolyte with $LiMn_2O_4$ cathode.

and phosphorous are increased (Table 1). The change in surface composition is attributed to the reduction products of electrolyte, such as lithium alkyl carbonates, polycarbonates, and lithium fluoride and the formation of an SEI [1].

The peaks of graphite and PVdF are weak while peaks characteristic of (C=O) containing species including lithium alkyl carbonates and polycarbonates are observed at ~289.5 eV and C–O containing species such as carbonates and polyethers are observed at ~286.5 eV in the C 1s spectrum. The O 1s spectrum provides further support for the presence of C=O and C–O (531.5 eV and 533.5 eV, respectively) containing species. The peak of lithium fluoride (685.0 eV) is the major peak in the F 1s spectrum, although the peak characteristic of $Li_xPO_yF_z$ (686.9 eV) is also present. The P 2p spectrum provides further support for the presence of $Li_xPO_yF_z$ due to the observation of the characteristic peak at 134.2 eV.

Analysis of the surface of the anode after cycling in the presence of LiFOP electrolyte (1.2 M LiFOP in EC/EMC, 3:7, vol.), suggests that the concentrations of carbon and fluorine are decreased, while the concentrations of oxygen and phosphorous are increased (Table 1).

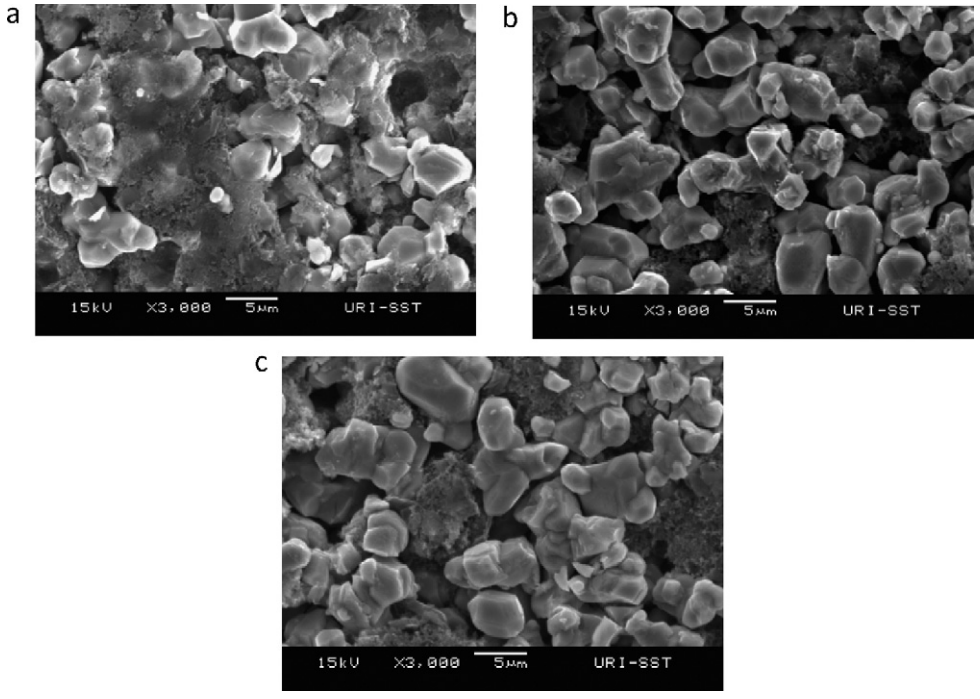

Fig. 9. SEM images of $LiMn_2O_4$ cathode (a) fresh, (b) cycled with $LiPF_6$ electrolyte and (c) cycled with LiFOP electrolyte.

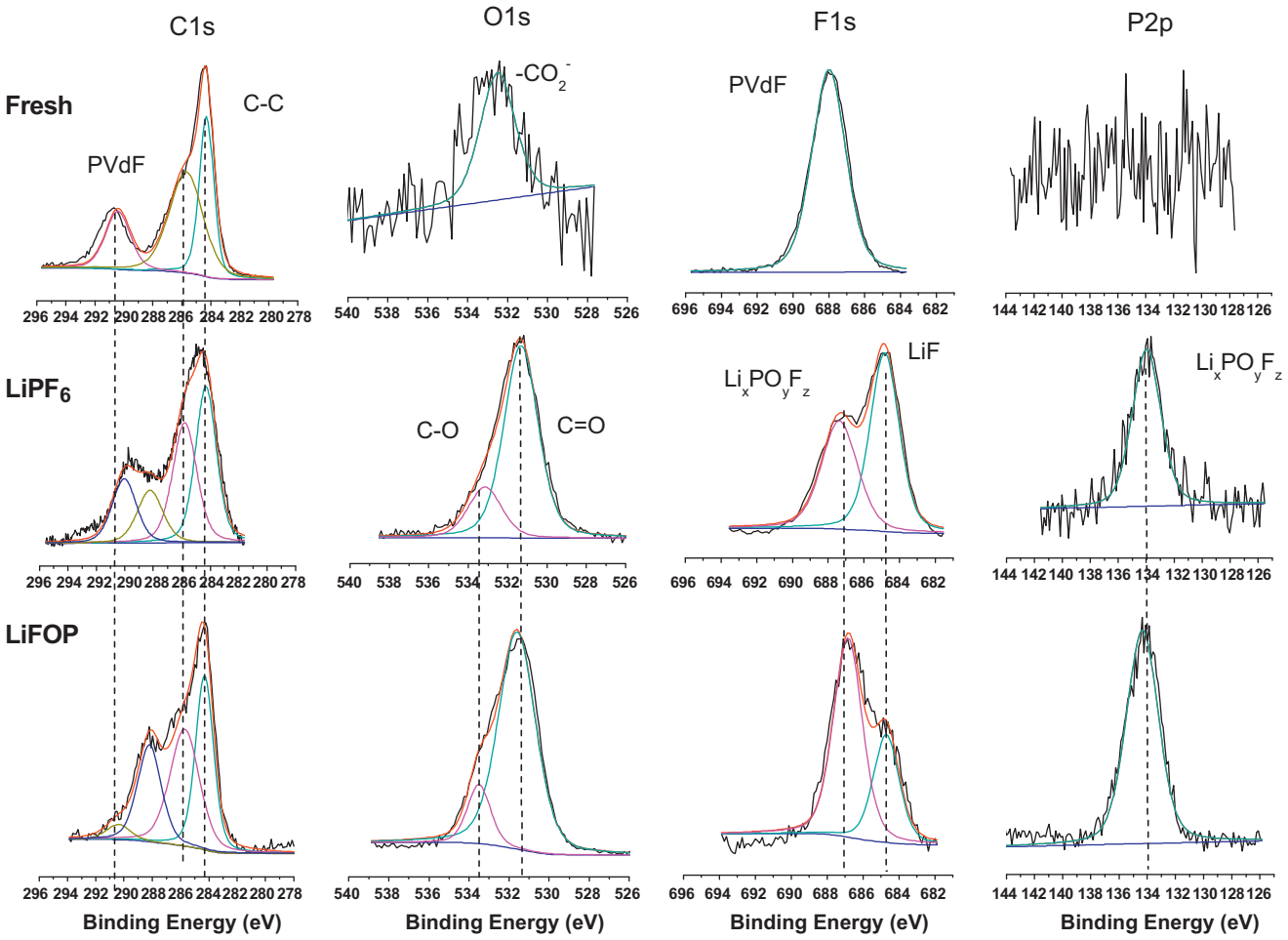

Fig. 10. XPS spectra of MCMB graphite anode used for $LiNi_{1/3}Co_{1/3}Mn_{1/3}O_2$ cathode (a) fresh, (b) cycled with $LiPF_6$ electrolyte and (c) cycled with LiFOP electrolyte.

The peaks of graphite and PVdF are weak while peaks characteristic of (C=O) containing species including lithium alkyl carbonates and polycarbonates are observed at ~289.5 eV and C–O containing species such as carbonates and polyethers are observed at ~286.5 eV in the C 1s spectrum. There are the corresponding peaks in the O 1s spectrum characteristic of C=O and C–O containing species including lithium alkyl carbonates, polycarbonates and oxalates at (531.5 eV) and (533.5 eV), respectively. The F 1s spectrum contains peaks corresponding to $Li_xPO_yF_z$ (686.9 eV) and lithium fluoride (685.0 eV), however, the intensity of the LiF peak is much weaker that that observed for the anode cycled with $LiPF_6$ electrolyte consistent with the lower concentration of F in Table 1. The P 2p spectrum contains a peak attributed to $Li_xPO_yF_z$ at 134.2 eV. The surface films on the anode cycled with the LiFOP electrolyte are similar to the surface films on the anodes cycled with $LiPF_6$ except there are higher concentrations of oxalate containing species as supported by the increased concentration of O and less LiF as supported by the lower concentration of F (Table 1).

The XPS spectra of $LiNi_{1/3}Co_{1/3}Mn_{1/3}O_2$ cathode (a) fresh; (b) cycled with $LiPF_6$ electrolyte; and (c) cycled with LiFOP electrolyte are provided in Fig. 11. There are three peaks in C 1s spectrum of the fresh $LiNi_{1/3}Co_{1/3}Mn_{1/3}O_2$ cathode characteristic of graphite at 284.3 eV and PVdF at 285.7 eV and 290.4 eV. There are two peaks in the O 1s spectrum, the peak of metal oxygen bond (M–O) at 529.4 eV and the peak of lithium carbonate at 531.6 eV. In the F 1s spectrum, a peak for PVdF is observed at 687.6 eV. The P 2p spectrum does not contain a peak. The Ni 2p, Co 2p and Mn 2p signal are also quite weak as previously reported for related samples [12].

Upon cycling in standard $LiPF_6$ electrolyte the surface of the cathode is modified (Table 2). The concentrations of C and P are increased while the concentrations of O, F, and the metals are decreased. The changes in the surface structure are consistent with the reaction of the electrolyte with the surface of the cathode materials.

Analysis of the cathode surface after 20 cycles with LiFOP electrolyte suggests that related changes are observed to the surface (Table 2). The changes in the concentration of C, F, P and the metals are less than the changes observed for $LiPF_6$ electrolyte. However, the concentration of O is significantly increased. The changes are consistent with the reaction of the electrolyte on the surface of the

Table 2
Elemental analysis of $LiNi_{1/3}Co_{1/3}Mn_{1/3}O_2$ cathode.

	C 1s (%)	O 1s (%)	F 1s (%)	P 2p (%)	Ni 2p (%)	Co 2p (%)	Mn 2p (%)
Fresh NMC	65.5	6.4	23.0	0	2.5	1.4	1.2
$LiPF_6$	80.9	4.2	12.2	0.7	1.6	0.2	0.2
LiFOP	58.0	15.9	19.3	2.2	2.2	0.9	1.5

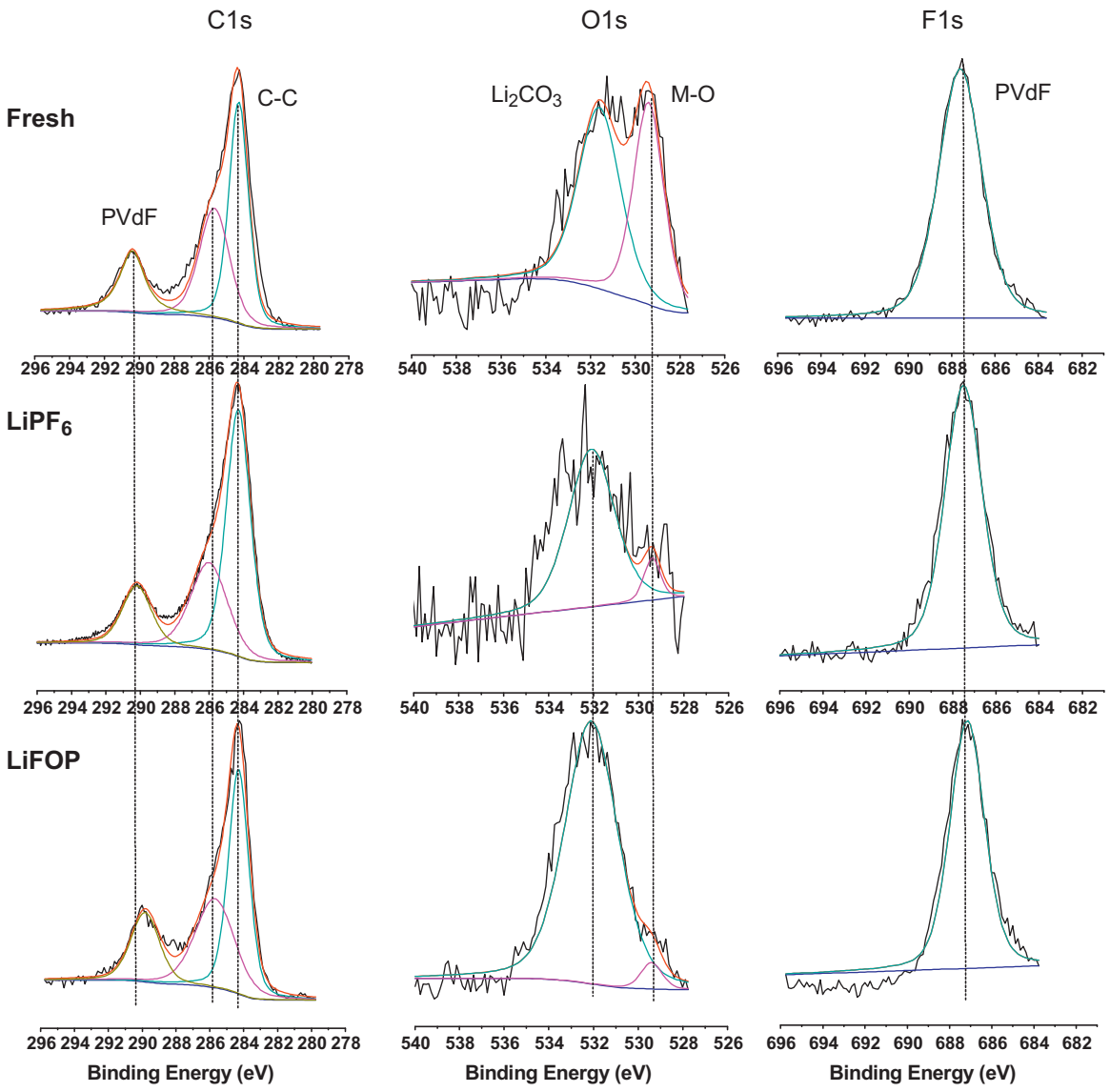

Fig. 11. XPS spectra of $LiNi_{1/3}Co_{1/3}Mn_{1/3}O_2$ cathode (a) fresh, (b) cycled with $LiPF_6$ electrolyte and (c) cycled with LiFOP electrolyte.

cathode materials and the deposition of O rich species including oxalates.

The XPS element spectra of the cathodes extracted from cells cycled with both the $LiPF_6$ and LiFOP electrolytes are quite similar (Fig. 11 (b) and (c)). The changes in the C 1s and F 1s spectra are very small while the O 1s spectra suggest a decrease in the peak of metal oxygen bond (M–O) at 529.4 eV and an increase in the concentration of C–O and C=O species at 531–532 eV consistent with the deposition of carbonates or oxalates. The intensity of the M–O peak is slightly greater for the cathode cycled with LiFOP electrolyte consistent with a thinner cathode surface film.

The XPS element spectra of NG anodes before and after cycling with a $LiFePO_4$ cathode with either $LiPF_6$ in EC/EMC (3:7, vol.) or LiFOP in EC/EMC (3:7, vol.) are depicted in Fig. 12 and the elemental concentrations are summarized in Table 3. The fresh anode is primarily composed of C (90.1%) with a low concentration of O (9.9%) due to the carboxymethyl starch (CMS) binder. The C 1s spectrum is dominated by the peak characteristic of graphite at 284.3 eV. The peak at 532.5 eV in O 1s spectrum is the characteristic peak of the CMS binder. There are no peaks observed in the F 1s and P 2p spectra.

The surface of the anode is modified after cycling with 1.2 M $LiPF_6$ in EC/EMC (3:7, vol.). The concentration of carbon is dramatically decreased, while the concentrations O and F are increased. There is also a small increase in the concentration of P. Analysis of the C 1s spectrum reveals that the peaks of graphite (284.3 eV) are very small while peaks characteristic of (C=O) containing species including lithium alkyl carbonates and polycarbonates are observed at ~289.5 eV and C–O containing species such as carbonates and polyethers are observed at ~286.5 eV. There is also evidence for C=O containing species (531.5 eV) and C–O containing species at 533.5 eV in the O 1s spectrum. The C 1s and O 1s peaks are consistent with the formation of a stable anode SEI. In the F 1s spectrum, the peak of lithium fluoride (685.0 eV) is the major peak,

Table 3
Elemental analysis of NG anode used for $LiFePO_4$ cathode.

	C 1s (%)	O 1s (%)	F 1s (%)	P 2p (%)
Fresh NG	90.1	9.9	0	0
$LiPF_6$	42.5	40.5	16.4	0.6
LiFOP	41.1	44.4	12.2	2.3

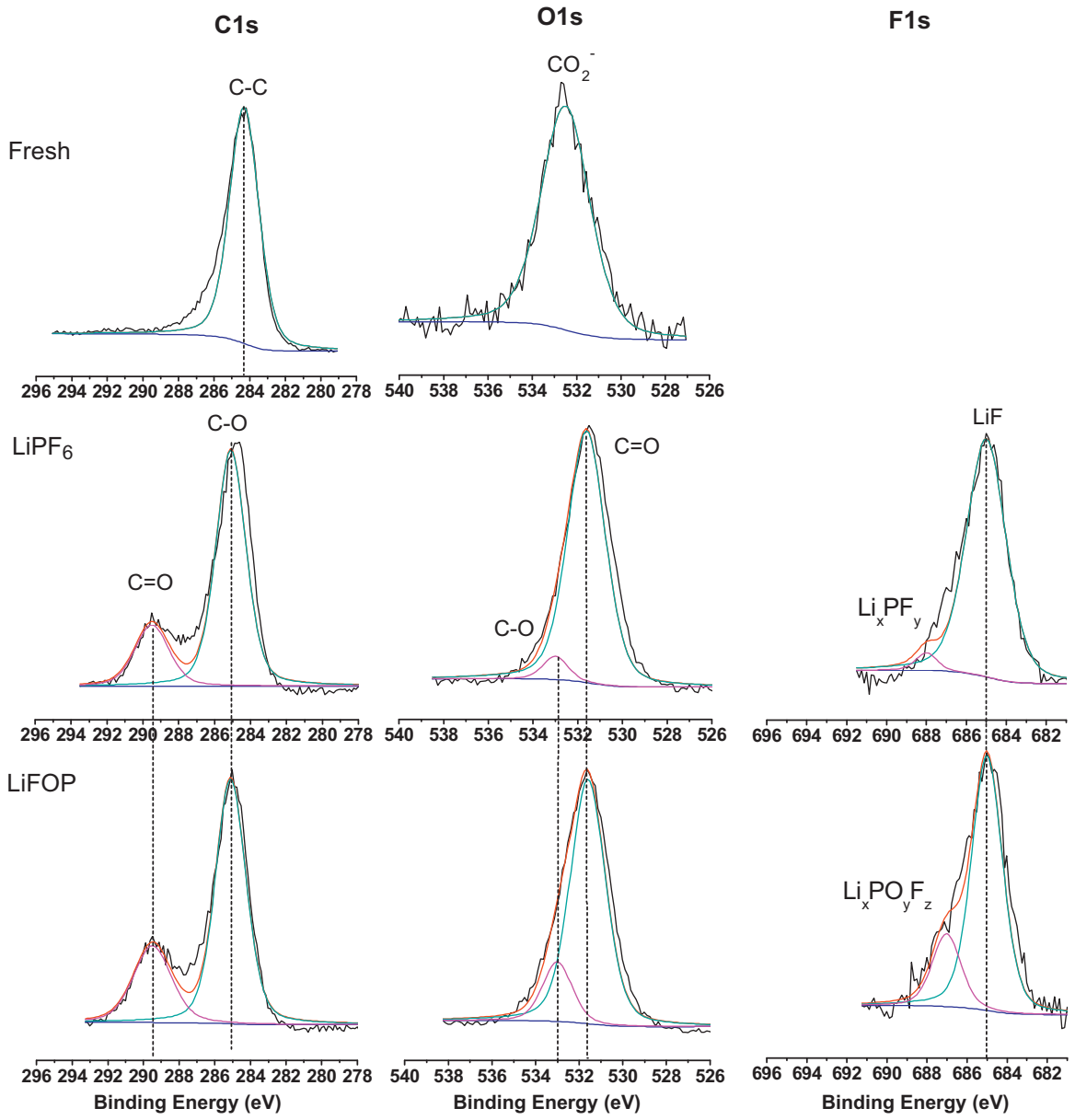

Fig. 12. XPS spectra of natural graphite anode used for $LiFePO_4$ cathode (a) fresh, (b) cycled with $LiPF_6$ electrolyte and (c) cycled with LiFOP electrolyte.

while the peak of $Li_xPF_yO_z$ (688–689 eV) is much smaller. There is also a small peak characteristic of $Li_xPF_yO_z$ observed in the P 2p spectrum at 136.7 eV.

Surface analysis of the anode cycled with LiFOP electrolyte is very similar to surface analysis of the anode cycled in $LiPF_6$ electrolyte, except the intensity of the $Li_xPF_y/Li_xPO_yF_z$ peaks at 686.9 eV in F 1s spectrum and 134.2 eV in P 2p spectrum have greater intensity. The similar surface species are consistent with the similar cycling performances for these electrode electrolyte combinations.

The XPS element spectra of $LiFePO_4$ cathodes, fresh and extracted from cells cycled with $LiPF_6$ in EC/EMC (3:7, vol.) or LiFOP in EC/EMC (3:7, vol.), are depicted in Fig. 13 and the elemental concentrations are summarized in Table 4. Analysis of the fresh $LiFePO_4$ cathode indicates the presence of three peaks in the C 1s spectrum. The peaks are characteristic of graphite at 284.3 eV and PVdF at 285.7 eV and 290.4 eV. The O 1s and P 2p spectra are dominated by the peaks of phosphorous oxygen bond (P–O) in $LiFePO_4$ at 531.16 eV, and 133.2 eV, respectively. The F 1s spectrum contains a single peak characteristic of PVdF at 687.6 eV. While there is significant noise in the Fe 2p spectrum, the peaks of Fe–O are observable.

Cycling in the presence of $LiPF_6$ electrolyte results in small changes to the surface of the cathode particles as summarized in Table 4. The concentrations of C, O and F are increased slightly while the concentrations of P and Fe are decreased. The changes in concentration are accompanied by small changes in the element spectra. The changes in the C 1s and O 1s spectra suggest an increase in the presence of C–O and C=O containing species, consistent with the deposition of electrolyte decomposition products on the cathode surface. Cycling with 1.2 M LiFOP in EC/EMC (3:7, vol.)

Table 4
Elemental analysis of $LiFePO_4$ cathode.

	C 1s (%)	O 1s (%)	F 1s (%)	P 2p (%)	Fe 2p (%)
Fresh $LiFePO_4$	53.2	18.4	19.5	4.8	4.1
$LiPF_6$	56.2	19.6	20.1	2.9	1.2
LiFOP	46.5	23.8	24.4	4.2	1.1

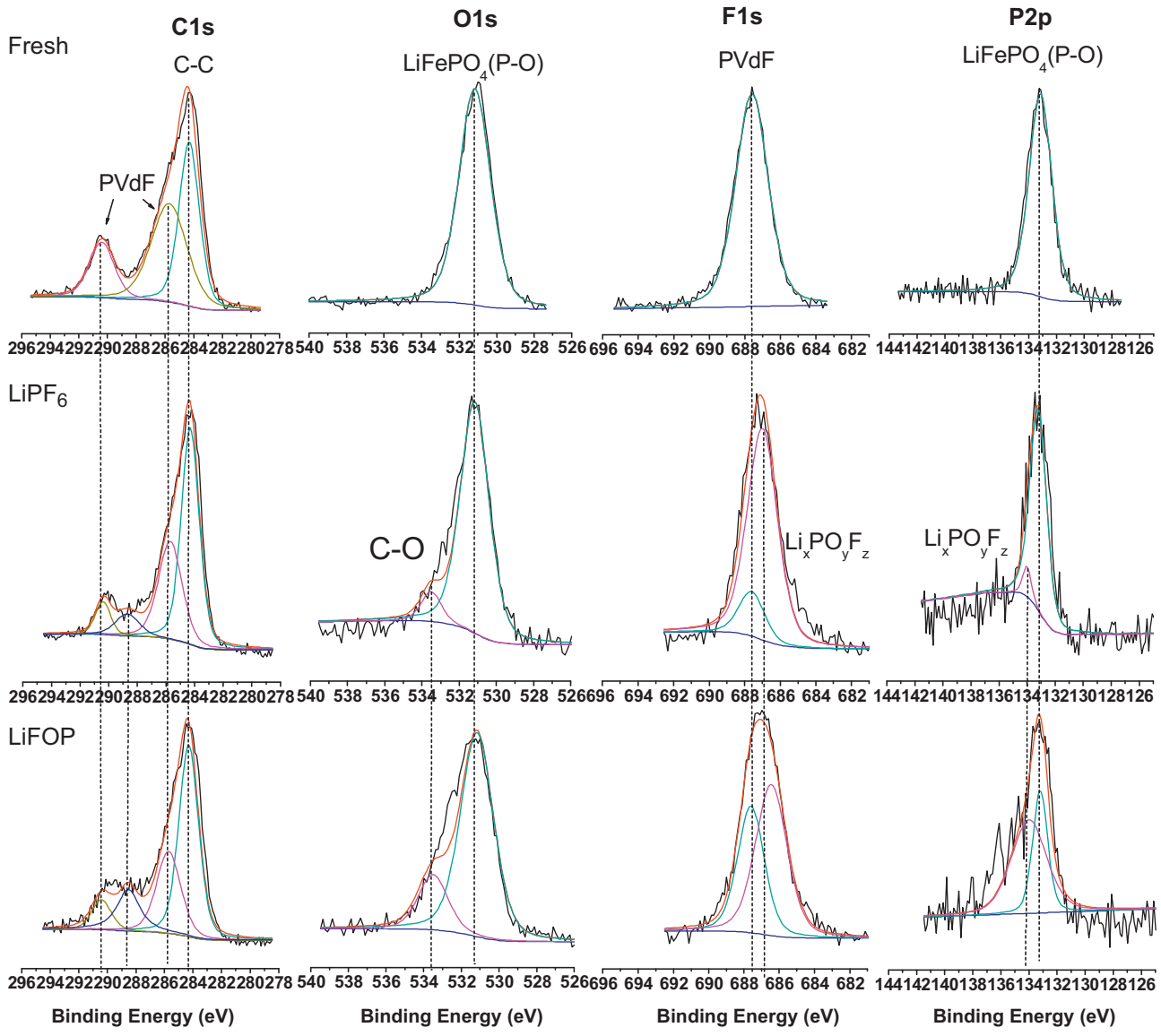

Fig. 13. XPS spectra of $LiFePO_4$ cathode (a) fresh, (b) cycled with $LiPF_6$ electrolyte and (c) cycled with LiFOP electrolyte.

provides related changes to the cathode surface consistent with the deposition of electrolyte decomposition products. However, the concentration of the C–O and C=O species appear to be greater in cells cycled with LiFOP consistent with a thicker surface film on the cathode. There is also evidence for the presence of $Li_xPO_yF_z$ species in the F 1s and P 2p spectra.

Surface analysis of the MCMB graphite before cycling and after cycling with a $LiMn_2O_4$ cathode $LiPF_6$ electrolyte or LiFOP electrolyte is provided in Fig. 14. Elemental analysis suggests that the MCMB surface contains C, F and O (Table 5). There are three peaks in C 1s spectrum of fresh MCMB anode, graphite at 284.3 eV and PVdF at 285.7 eV and 290.4 eV. The peak at 532.5 eV in O 1s spectrum is the characteristic peak of surface oxidation (CO_2^-) while the peak at 687.6 eV in the F 1s spectrum is consistent with PVdF.

Cycling the cell with $LiPF_6$ results in changes to the surface of the anode (Table 5). The concentration of C is dramatically decreased, with an increase in concentration of O and F. The changes are consistent with the generation of an SEI on the anode. The C 1s peaks of graphite and PVdF are weak while peaks characteristic of (C=O) and (C–O) containing species at 289.5 and 286.5 eV, respectively, are strong and consistent with the formation of lithium alkyl carbonates, polycarbonates, and polyethers. The O 1s spectra also contain evidence for C=O (531.5 eV) and C–O (533.5 eV) containing species. The F 1s spectrum, is dominated by the peak characteristic of LiF (685.0 eV) with a smaller peak which is likely a combination of PVDF and $Li_xPF_yO_z$ (687–688 eV). The XPS data is consistent with the formation of an anode SEI containing the reduction products of the electrolyte, such as lithium alkyl carbonates, polycarbonates, lithium fluoride, and lithium fluorophosphates.

Similar changes to the anode surface are observed by XPS upon cycling with LiFOP electrolyte. The concentration of carbon on the surface of the anode decreases from 76.1% to 37.8%, compared to the fresh electrode. While the change in concentration is similar

Table 5
Elemental analysis of MCMB graphite anode used for $LiMn_2O_4$ cathode.

	C 1s (%)	O 1s (%)	F 1s (%)	P 2p (%)
Fresh MCMB	76.1	1.1	22.8	
$LiPF_6$	39.3	46.2	14.4	
LiFOP	37.8	36.5	19.9	5.72

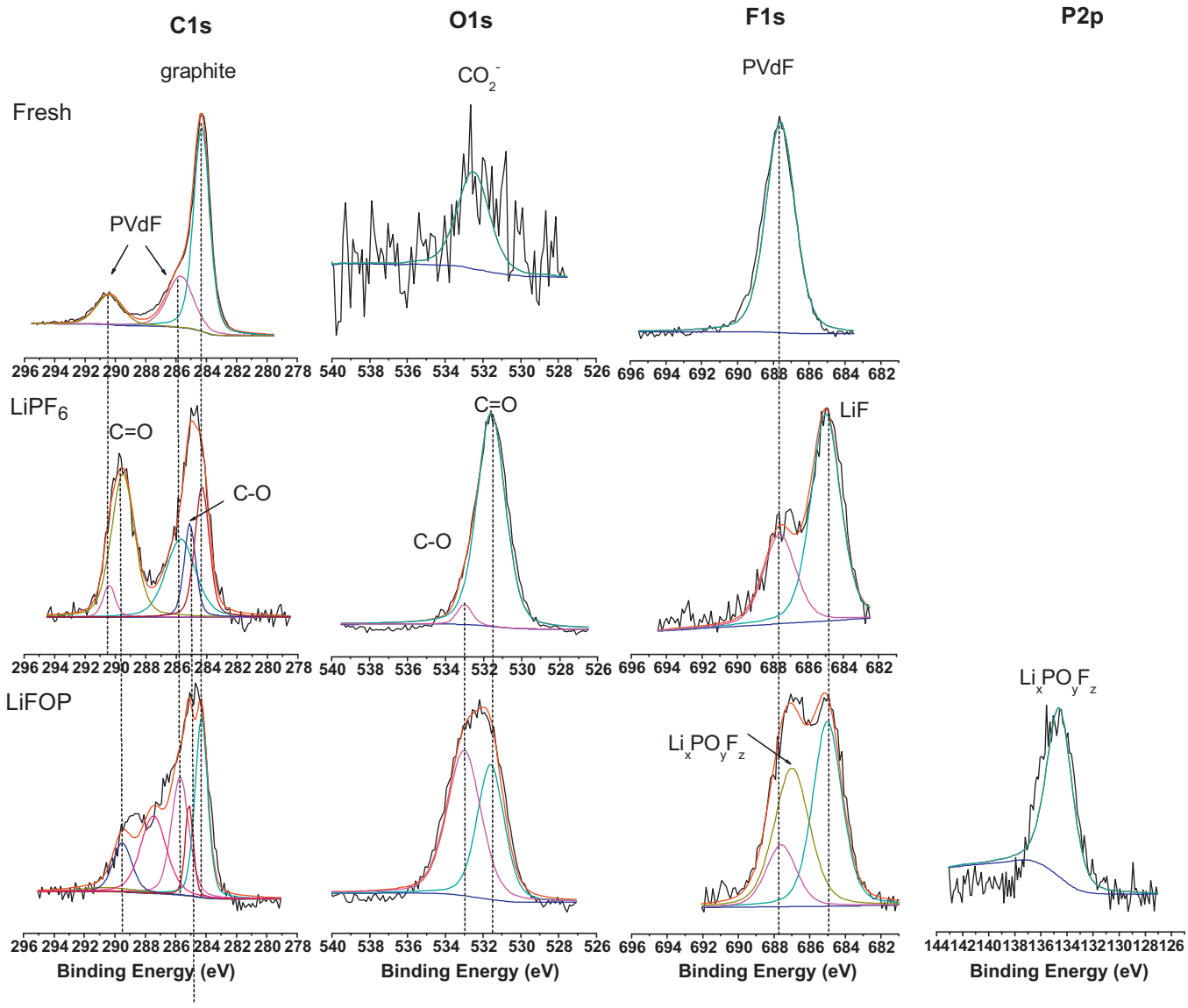

Fig. 14. XPS spectra of MCMB anode used for $LiMn_2O_4$ cathode (a) fresh, (b) cycled with $LiPF_6$ electrolyte and (c) cycled with LiFOP electrolyte.

to that observed with the $LiPF_6$ electrolyte, the element spectra are quite different. The peak characteristic of C=O at ~289.5 eV is smaller with LiFOP electrolyte while there is a increase in the intensity at ~287.5 eV consistent with the presence of oxalate containing species. A similar difference is observed in the O 1s XPS spectrum. The peak at 531.5 eV (C=O) is the dominant peak in the O 1s spectra of the anode cycled with $LiPF_6$ electrolyte, while the peak at 531.5 eV is a minor peak in the O 1s spectra of the anode cycled with LiFOP electrolyte. In addition, the peaks at 686.9 eV in F 1s spectrum and 134.2 eV in P 2p spectrum characteristic of $Li_xPO_yF_z$ have much greater intensity for the anode cycled with LiFOP electrolyte. The differences in the structure of the anode SEI correlate with the different cycling behaviors of the different electrolytes.

Surface analysis of the fresh and cycled $LiMn_2O_4$ cathodes are depicted in Fig. 15 and summarized in Table 6. There are three peaks in C 1s spectrum of fresh cathode, graphite peak at 284.3 eV, peaks of PVdF at 285.7 eV and 290.4 eV, respectively. The peak at 529.8 eV in the O 1s spectrum is the characteristic peak of the manganese oxygen bond (Mn–O) on the surface of the electrode. The corresponding peak for the Mn–O bond is also observed in the Mn 2p spectra. A peak for PVdF is observed at 687.6 eV in the F 1s spectrum.

After cycling the cell with $LiPF_6$ electrolyte the elemental concentrations are slightly altered suggesting small changes to the surface. The concentration of C and Mn are slightly decreased while the concentrations of O, F and P are increased. The peak for the Mn–O bond (529.8 eV) is observed in the O 1s spectrum, but has weaker intensity. An additional peak is observed at 532.5 eV in the O 1s spectrum characteristic of polycarbonates or lithium alkyl carbonates. A related peak characteristic of C=O containing species is observed in the C 1s spectrum at 286.5 eV. The F 1s spectrum contains a large peak for PVdF (687.6 eV) and a small peak for LiF at 685.0 eV. The data suggests that a thin surface film is being generated on the cathode.

Table 6
Elemental analysis of $LiMn_2O_4$ cathode.

	C 1s (%)	O 1s (%)	F 1s (%)	P 2p (%)	Mn 2p (%)
Fresh $LiMn_2O_4$	59.9	12.8	19.4	0	7.9
$LiPF_6$	55.2	17.1	20.0	1.2	6.5
LiFOP	52.5	21.3	20.0	2.7	3.5

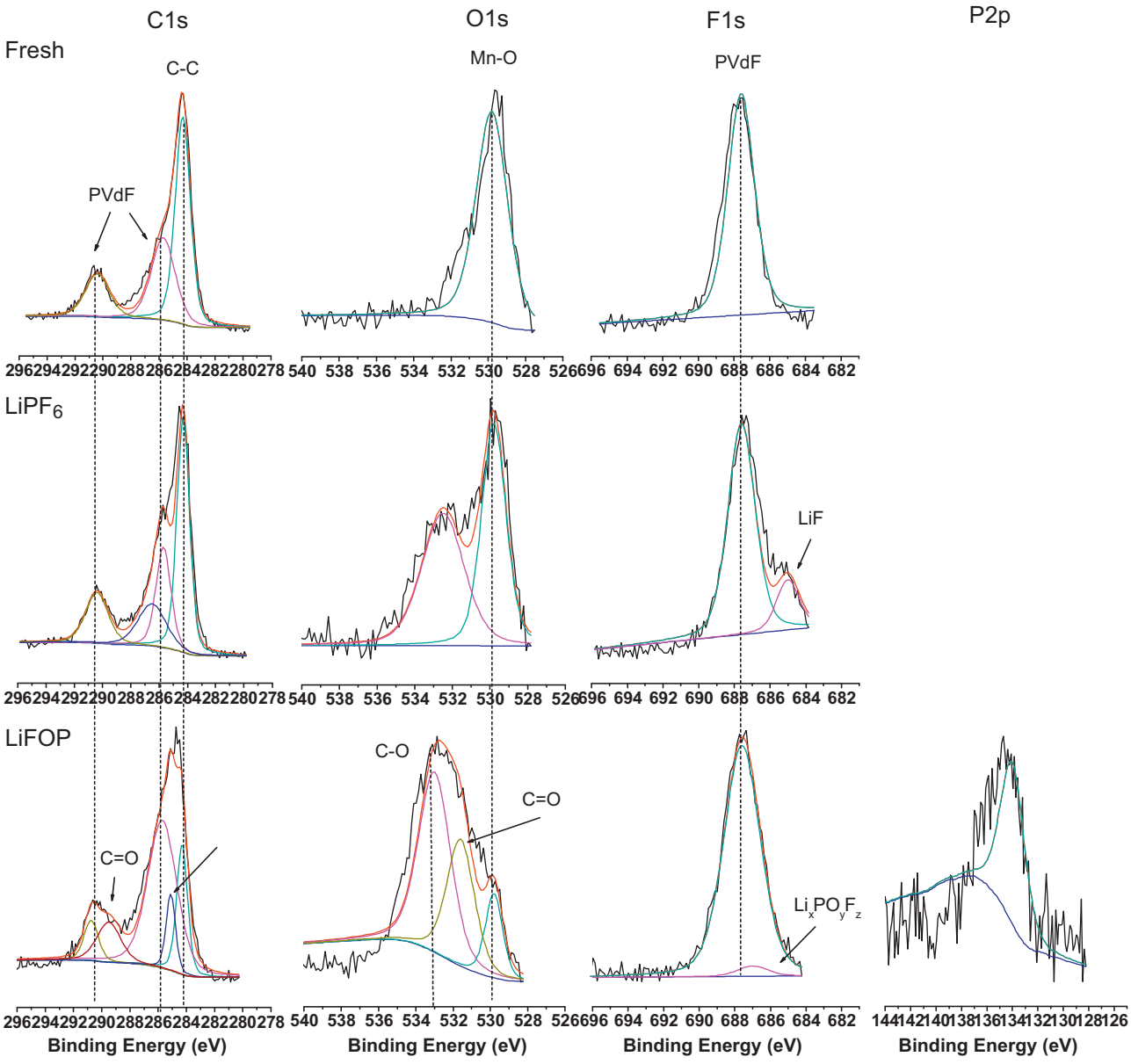

Fig. 15. XPS spectra of $LiMn_2O_4$ cathode (a) fresh, (b) cycled with $LiPF_6$ electrolyte and (c) cycled with LiFOP electrolyte.

Analysis of the cathode after cycling with LiFOP electrolyte suggests similar changes to the surface. However, the lower concentrations of C and Mn along with the higher concentrations of O, F, and P are consistent with thicker cathode surface films compared to cathode cycled with $LiPF_6$ electrolyte. In addition, the peak characteristic of Mn–O is very weak in the O 1s spectrum further supporting a thicker surface film composed of electrolyte decomposition products including lithium alkylcarbonates, polycarbonates, $Li_xPF_yO_z$, and oxalate containing species.

4. Conclusions

A comparison of $LiPF_6$ and LiFOP electrolytes was conducted for three different sets of paired electrodes: MCMB/$LiNi_{1/3}Co_{1/3}Mn_{1/3}O_2$, natural graphite/$LiFePO_4$, and MCMB/$LiMn_2O_4$. The formation cycle efficiencies and cycling performance during the first 25 cycles are very similar for $LiPF_6$ and LiFOP electrolytes for both MCMB/$LiNi_{1/3}Co_{1/3}Mn_{1/3}O_2$ and natural graphite/$LiFePO_4$ cells. Surface analysis of the electrodes after cycling suggests that the anode SEI and the cathode surface films are similar for $LiPF_6$ and LiFOP electrolytes, for the MCMB/$LiNi_{1/3}Co_{1/3}Mn_{1/3}O_2$ and natural graphite/$LiFePO_4$ cells.

The first cycle efficiencies are much lower for LiFOP electrolytes than $LiPF_6$ electrolytes for MCMB/$LiMn_2O_4$ cells. Ex-situ surface analysis of the electrodes extracted from MCMB/$LiMn_2O_4$ cells suggests that the anode surface films are dependent upon the electrolyte while the cathode films are similar for both electrolytes. Thus the performance differences of the MCMB/$LiMn_2O_4$ cells cycled with the $LiPF_6$ and LiFOP electrolytes are due to the SEI forming reactions on the anode as opposed to the cathode. While we do not have a full understanding of the differences between the cycling performance of the MCMB/$LiNi_{1/3}Co_{1/3}Mn_{1/3}O_2$ and natural graphite/$LiFePO_4$ cells compared to the MCMB/$LiMn_2O_4$ cells, the data suggests that the differences are due to different types of graphite. While both $LiNi_{1/3}Co_{1/3}Mn_{1/3}O_2$ and $LiMn_2O_4$ cathodes were cycled against MCMB graphite anodes, the particle size of the different forms of MCMB are clearly evident in Figs. 4 and 8. We are conducting a more detailed analysis of the reactions of different graphite electrodes with $LiPF_6$ and LiFOP electrolytes and will present these results in due course.

Previous results confirm that carbonate solutions of LiFOP have comparable conductivity to carbonate solutions of $LiPF_6$ but LiFOP electrolytes have much better thermal stability [10,11]. The results presented in this manuscript provide further support that LiFOP is a potentially interesting alternative salt for lithium ion batteries. LiFOP electrolytes have good cycling performance in the presence of three of the most widely investigated cathode materials for lithium ion batteries, $LiNi_{1/3}Co_{1/3}Mn_{1/3}O_2$, $LiFePO_4$, and $LiMn_2O_4$. The stable cycling performance and cathode surface analysis confirm compatibility with all three cathode materials. While previous investigations indicated LiFOP reduction on the surface of the graphitic anode led to reduced reversible capacity during the formation cycles, the results presented in this study indicate that the first cycle irreversible capacity is dependent upon the type of graphite used and that proper matching of graphitic anode to the LiFOP electrolyte can lead to comparable cycling performance to $LiPF_6$ electrolytes.

Acknowledgement

We thank the Batteries for Advanced Transportation Technologies (BATT) Program supported by the U.S. Department of Energy Office of Vehicles Technologies for financial support of this research.

References

[1] K. Xu, Chem. Rev. 104 (2004) 4303.
[2] A.M. Andersson, D.P. Abraham, R. Haasch, S. MacLaren, J. Liu, K. Amine, J. Electrochem. Soc. 149 (2002) A1358.
[3] M. Herstedt, D.P. Abraham, J.B. Kerr, K. Edstrom, Electrochim. Acta 49 (2004) 5097.
[4] B. Ravdel, K.M. Abraham, R. Gitzendanner, J. DiCarlo, B.L. Lucht, C. Campion, J. Power Sources 119–121 (2003) 805.
[5] C. Campion, W. Li, W.B. Euler, B.L. Lucht, B. Ravdel, J. Dicarlo, R. Gitzendanner, K.M. Abraham, Electrochem. Solid-State Lett. 7 (2004) A194.
[6] S.S. Zhang, J. Power Sources 162 (2006) 1379.
[7] W. Xu, C.A. Angell, Electrochem. Solid-State Lett. 4 (2001) E1.
[8] K. Xu, S. Zhang, B.A. Poese, T.R. Jow, Electrochem. Solid-State Lett. 5 (2002) A259.
[9] A. Xiao, L. Yang, B.L. Lucht, Electrochem. Solid-State Lett. 10 (2007) A241.
[10] M. Xu, A. Xiao, W. Li, B.L. Lucht, Electrochem. Solid-State Lett. 12 (2009) A155.
[11] M. Xu, A. Xiao, W. Li, B.L. Lucht, J. Electrochem. Soc. 157 (2010) A115.
[12] W. Li, B.L. Lucht, J. Electrochem. Soc. 153 (2006) A1617.